

Supplemental Information for:

Low Valent Phosphorus in the Molecular Anions $[P_5Se_{12}]^{5-}$ and $\beta-[P_6Se_{12}]^{4-}$: Phase Change Behavior and Near Infrared Second Harmonic Generation of $Cs_5P_5Se_{12}$

In Chung,^{a,b} Joon I. Jang^c Matthew A. Gave,^a David P. Weliky,^a and Mercouri G. Kanatzidis*^{a,b}

Contents

Experimental Details of ^{31}P Solid-state NMR.

Experimental Details of X-ray photoelectron spectroscopic analysis.

S1. ^{31}P Solid-state NMR of $Cs_4P_6Se_{12}$.

S2. ^{31}P Solid-state NMR of $Cs_4P_6Se_{12}$.

S3. ^{31}P Solid-state NMR of $Cs_5P_5Se_{12}$.

S4. ^{31}P Solid-state NMR of $Cs_5P_5Se_{12}$.

S5. X-ray Photoelectron Spectroscopy of $Cs_4P_6Se_{12}$.

S6. DTA, Powder XRD, Raman, and Electronic Absorption Spectra of Crystalline and Glassy $Cs_5P_5Se_{12}$.

S7. Raman and Electronic Absorption Spectra of Crystalline and Glassy $Cs_4P_6Se_{12}$.

S8. SHG response of $Cs_5P_5Se_{12}$.

S9. Selected Bond Distances and Angles for $Cs_5P_5Se_{12}$ and $Cs_4P_6Se_{12}$.

Experimental Details

³¹P Solid-state NMR Spectroscopy

Room temperature ³¹P NMR spectra were collected on a 9.4 T spectrometer (Varian Infinity Plus) using a Varian Chemagnetics double resonance magic angle spinning (MAS) probe. The sample volume in the 4 mm diameter zirconia rotors was ~50 µL and the MAS frequency was 14 KHz. Each sample was ground to a fine powder before being packed in the rotor. The π/2 pulse width was 5.55 µs and was calibrated using H₃PO₄. Spectra were processed using 50 Hz line broadening and up to a 10th order polynomial baseline correction. Longitudinal relaxation times (*T*₁) were determined as described elsewhere.¹

X-ray Photoelectron Spectroscopy

Single crystals of Cs₅P₅Se₁₂ and Cs₄P₆Se₁₂ were ground to powders and pressed to pellets. X-ray photoelectron spectroscopy (XPS) analyses were performed on the pellets with Omicron ESCA probe equipped with EA 125 energy analyzer. Photoemission was stimulated by a monochromated Al *K*α radiation (1486.6 eV). Binding energies were normalized to the C 1s binding energy set at 285.0 eV. To analyze the XPS results, linear background correction was applied and photolines were fit by Gaussian-Lorentzian curves. The fitted curve was deconvoluted to reveal multiple valence states of phosphorus and their 2p_{1/2} and 2p_{2/3} spectra. The quantitative analysis of P in Cs₅P₅Se₁₂ and Cs₄P₆Se₁₂ were carried out by XPS using the integrated areas of the core-level peaks of P 2p.

XPS analysis for both Cs₅P₅Se₁₂ and Cs₄P₆Se₁₂ showed the presence of two different oxidation states of phosphorus. Since the higher binding energy results from the higher oxidation state of a corresponding element in principle, the spectra found in the higher region can be assigned to P⁴⁺ and those in the lower region to P³⁺ for Cs₅P₅Se₁₂ and P²⁺ for Cs₄P₆Se₁₂. Area ratio of respective spectrum from higher and lower oxidation states was integrated to give 4.1 for Cs₅P₅Se₁₂ and 1.9 for Cs₄P₆Se₁₂, which agrees well with structural analysis model of Cs₅[P²⁺(P⁴⁺)₂Se₆)₂] and Cs₄[(P²⁺)₂(P⁴⁺)₂Se₆)₂].

Cs₄P₆Se₁₂ ³¹P Solid State NMR

The NMR spectrum of Cs₄P₆Se₁₂ is displayed in Figure S1. The peak at 95.5 ppm can be assigned to the P(3) atoms, and the peak at 65.5 ppm can be assigned to the P(1) and P(2) atoms. The P(1) and P(2) chemical environments are very similar, and the bond lengths and angles for each nearly agree within the error of the crystallographic refinement. It is therefore possible that the chemical shifts corresponding to these atoms overlap, thus accounting for the observed 1:2 ratio of the spectral peaks. The 95.5 ppm and 65.5 ppm spectral features appear as doublets with coupling constants J = 250 and J = 270 Hz, respectively. One possible assignment of these splittings is two bond P-P J-coupling. Two bond P-P scalar coupling in the solution phase have been observed with

coupling constants of ~ 300 Hz.^{5,6} However, other compounds such as KBiP_2S_7 ^{2,3} and $\text{Rb}_4\text{P}_6\text{Se}_{12}$ ⁴ contained inequivalent ^{31}P atoms separated by two bonds and two bond P-P coupling was not observed.

Another possible assignment is that the 95.5 and 65.5 ppm peaks correspond to the P(1) and P(2) atoms and the observed splitting is one-bond P(1)-P(2) J coupling. In this assignment, the P(3) signal was not detected. It is noted that the 95.5 and 65.5 ppm peaks were the only significant isotropic peaks observed under the conditions of a 5000 s delay between acquisitions and a 1200 ppm spectral window. One weakness in this assignment is that the 95.5/65.5 ppm intensity ratio is <1.

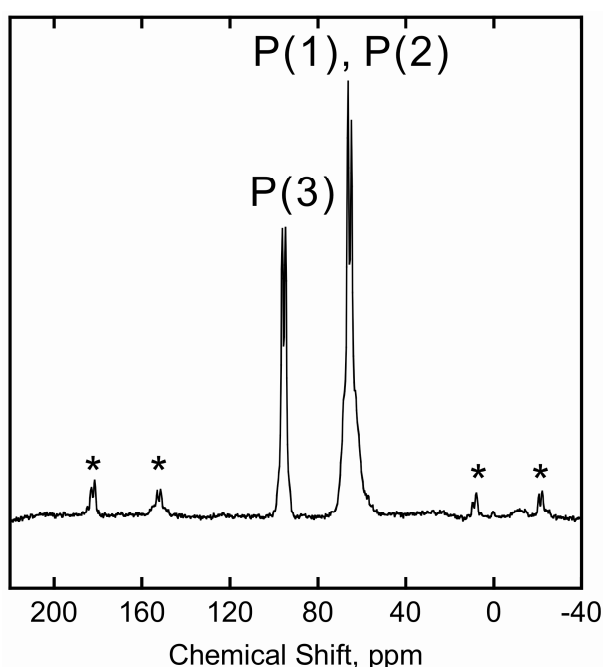


Figure S1. ^{31}P NMR Spectrum of $\text{Cs}_4\text{P}_6\text{Se}_{12}$ at a 14 KHz MAS frequency. The peak centered at 95.5 ppm was a doublet and had splittings with $J = 250$ Hz and the peak centered at 65.5 ppm was also a doublet and had splittings with $J = 270$ Hz. The peaks had approximately a 1:2 intensity ratio. The peak centered at 95.5 ppm had a longitudinal relaxation time of 2600 s, and the peak centered at 65.5 ppm had a longitudinal relaxation time of 1900 s. The weaker signals (*) above 120 ppm and below 40 ppm are the spinning sidebands of the 65.5 and 95.5 ppm isotropic peaks.

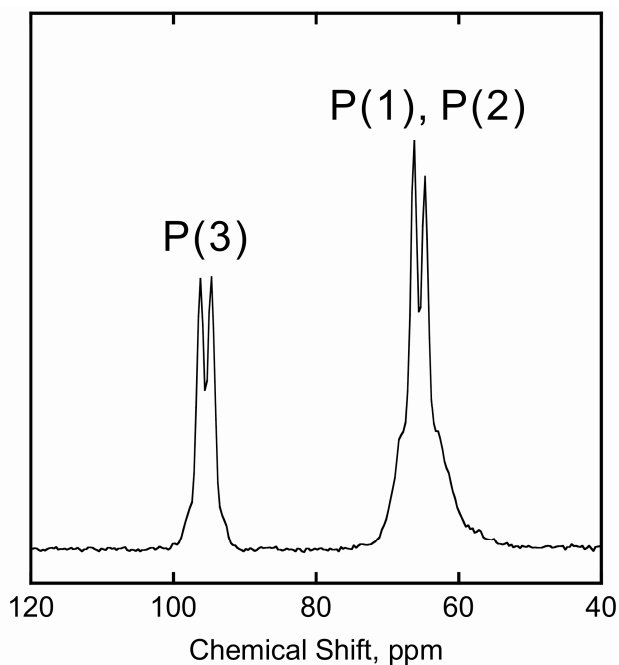


Figure S2. The two doublets centered at 95.5 and 65.5 ppm from Figure S1. are represented.

$Cs_5P_5Se_{12}$ ^{31}P Solid State NMR

The ^{31}P NMR of $Cs_5P_5Se_{12}$ is displayed in Figure S2. The difference in bond lengths and angles between the P(1) and P(2) coordination environments is significantly outside of the range of the error in the crystallographic refinement, and therefore distinct chemical shifts resulting from each of these sites are predicted. Including the signal from the P(3) atom, there should therefore be three peaks in the NMR spectrum. One possible assignment is that the two doublets centered at 63.1 ppm and 48.7 ppm can be attributed to the P(1) and P(2) nuclei and the singlet at 16.1 ppm can be attributed to the P(3) nucleus. There are twice as many P(1) and P(2) atoms per formula unit than P(3) atoms, so the spectral intensity of the peaks corresponding to P(1) and P(2) should be twice that of P(3). The spectral intensity of the 63.1 ppm and 48.7 ppm peaks is \sim 3.5 and \sim 2.5-fold greater than the 16.1 ppm peak, respectively. The peak at 94.9 ppm is likely due to $Cs_4P_6Se_{12}$ impurity in the sample and this impurity would also result in a 65.5 ppm peak which would be unresolved from the 63.1 ppm peak of $Cs_5P_5Se_{12}$. The $Cs_4P_6Se_{12}$ impurity could therefore account for some of the discrepancy between the observed and predicted intensities of this assignment. The splitting of the 63.1 and 48.7 ppm peaks is attributed to one-bond P-P coupling between the crystallographically inequivalent P(1) and P(2) atoms. The two bond P(1)-P(3) or P(2)-P(3) scalar coupling was not observed.

Previously, P^{4+} in selenophosphate anions with P-P bonds were observed to have positive ^{31}P chemical shifts, and P^{5+} in selenophosphate anions without P-P bonds were observed to have negative ^{31}P chemical shifts.⁷ The chemical shift of the non P-P bonded

P^{3+} atom in this compound, namely P(3), was assigned to a spectral feature with a positive chemical shift.

The longitudinal relaxation times were $\sim 600(100)$, 70(10), and 10(3) s for the 63.1, 48.7, and 16.1 ppm features, respectively. The latter two values are somewhat shorter than those of typical selenophosphates.¹ Phosphorus-containing compounds with multiple crystallographically unique ${}^3\text{P}$ sites typically do not have such a wide range of longitudinal relaxation times for the ${}^3\text{P}$ sites.

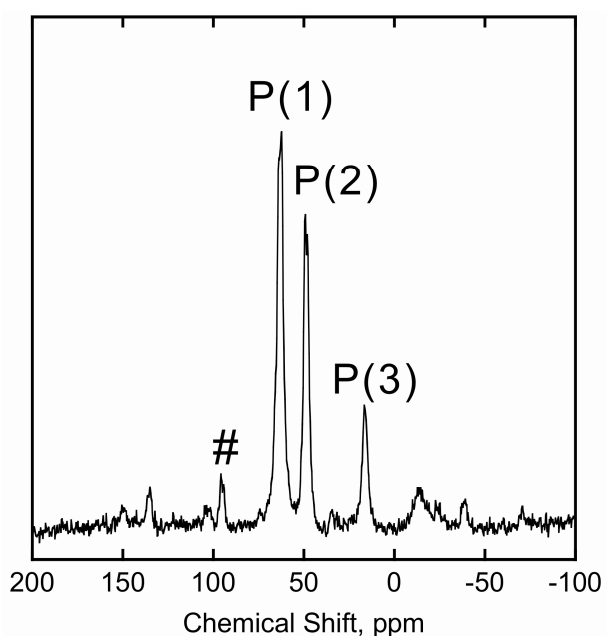


Figure S3. ${}^3\text{P}$ NMR Spectrum of $\text{Cs}_5\text{P}_5\text{Se}_{12}$ at a 14 KHz MAS frequency. The peak centered at 63.1 ppm was a doublet with a splitting of $J = 200$ Hz, the peak centered at 48.7 ppm was a doublet with a splitting of $J = 200$ Hz and the peak at 16.1 ppm was a singlet. The peaks had approximately a 7:5:2 intensity ratio. # denotes impurity, possibly $\text{Cs}_4\text{P}_6\text{Se}_{12}$.

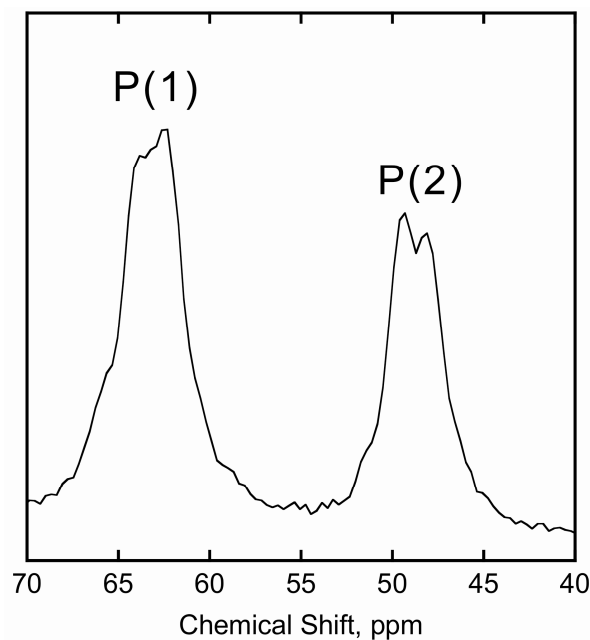


Figure S4. The two doublets centered at 63.1 and 48.1 ppm from Figure S1. are represented.

Figure S5. X-ray photoelectron spectrum, peak fitting, and deconvolution profiles in the P 2p region of $\text{Cs}_4\text{P}_6\text{Se}_{12}$.

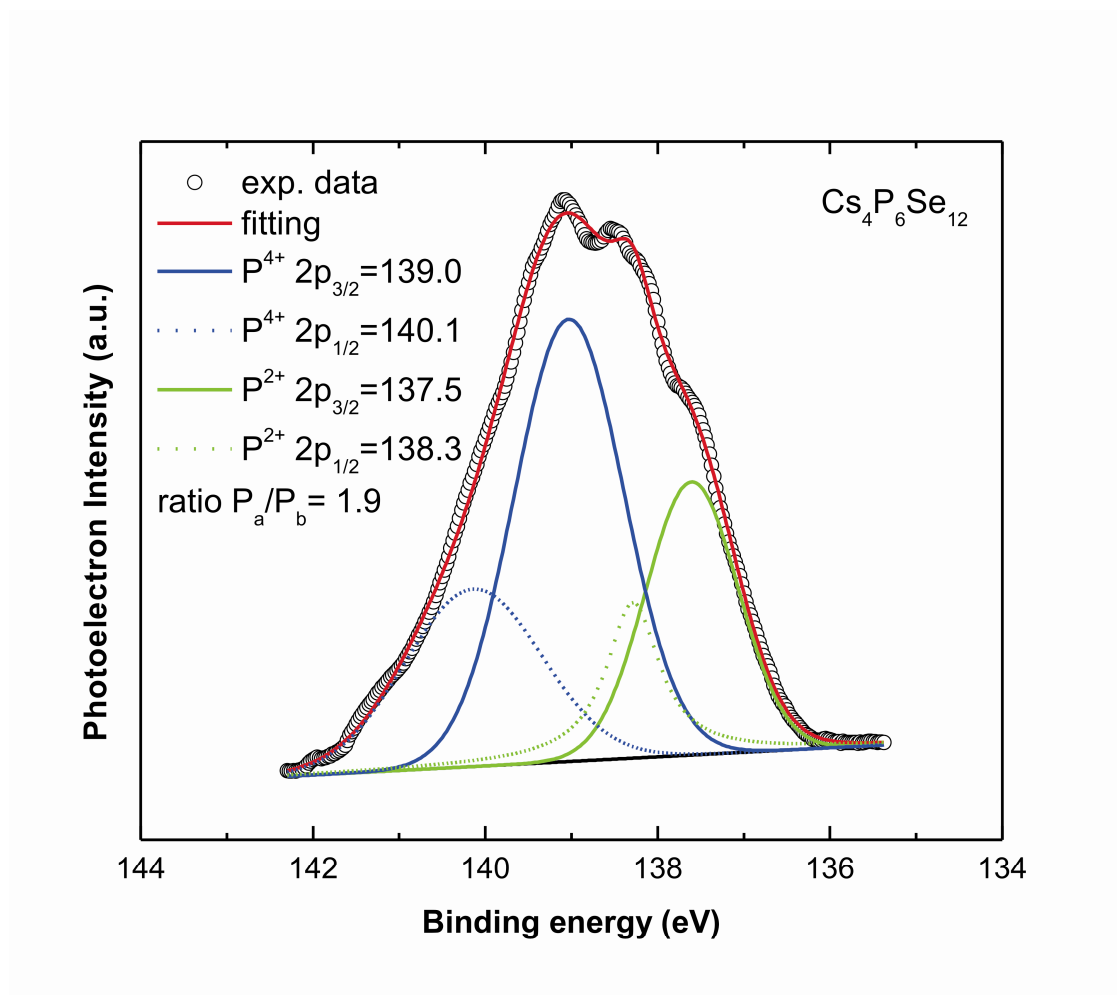


Figure S6. (a) Differential thermal analysis diagrams of $\text{Cs}_5\text{P}_5\text{Se}_{12}$ showing melting in the 1st cycle with no crystallization on cooling (upper black line). Glass crystallization is observed in the 2nd heating cycle. $\text{Cs}_5\text{P}_5\text{Se}_{12}$ is a pristine crystal at A, glass at B and restored crystal at C. (b) X-ray powder diffraction patterns of pristine (A), glassy (B) and recrystallized crystal(C). (c) The Raman and (d) the electronic absorption spectra of crystalline (black line) and glassy (red line) $\text{Cs}_5\text{P}_5\text{Se}_{12}$.

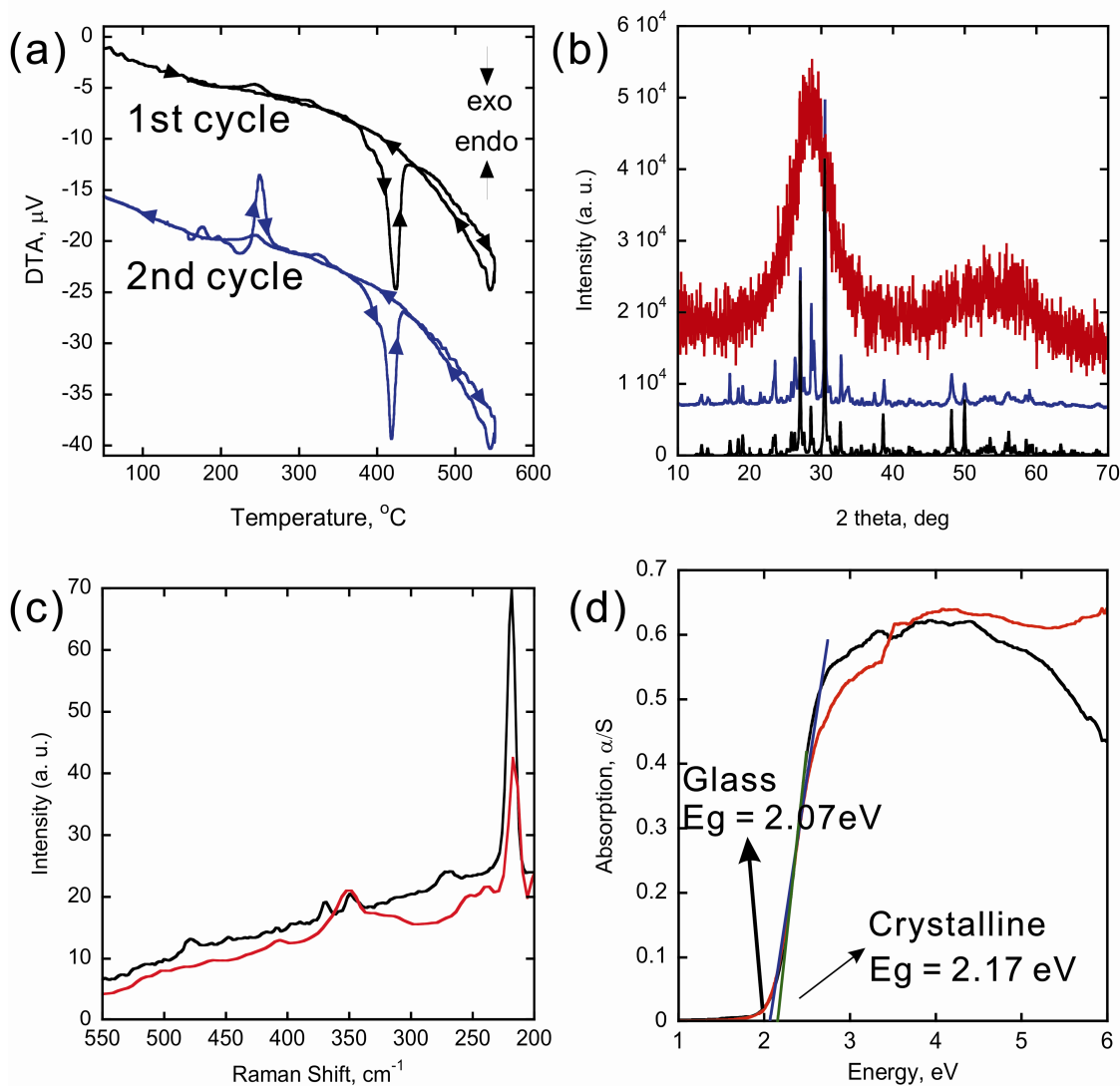


Figure S7. (a) The Raman and (b) the electronic absorption spectra of crystalline (black line) and glassy (red line) $\text{Cs}_5\text{P}_5\text{Se}_{12}$.

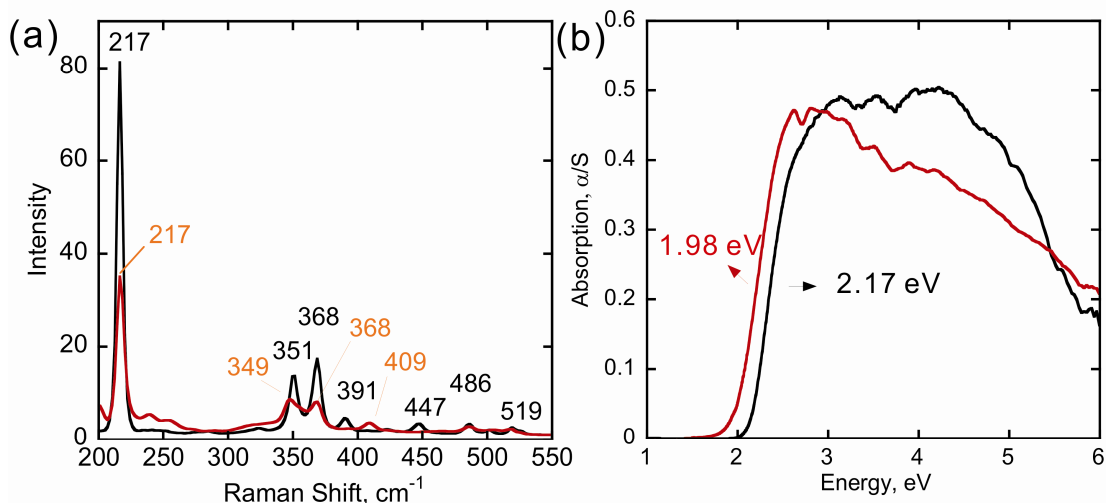
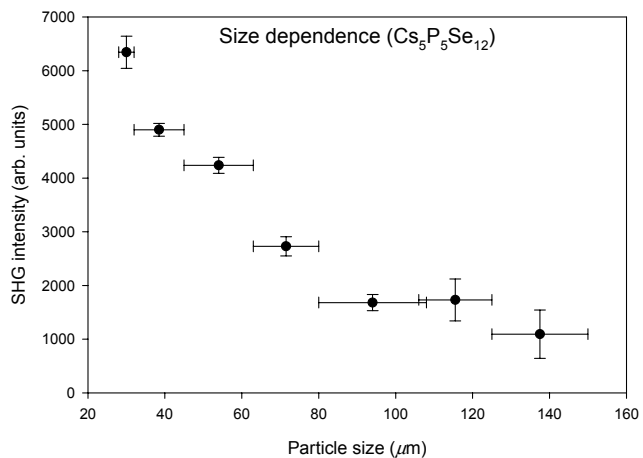
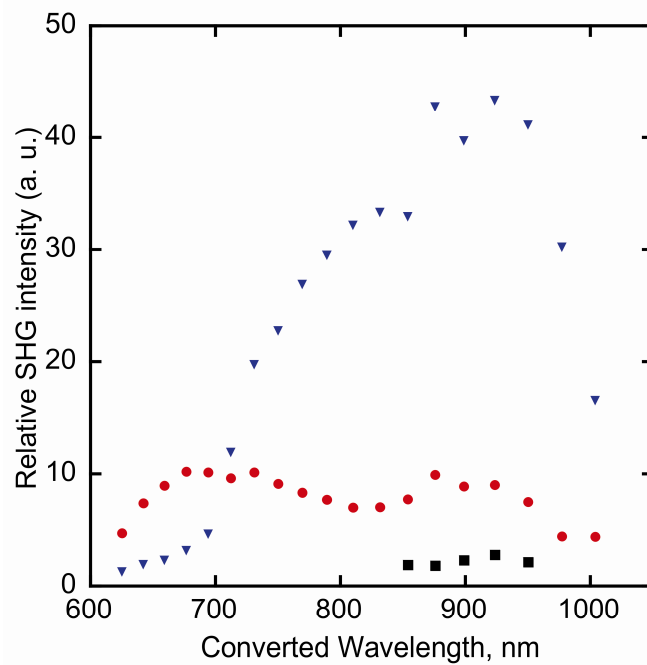


Figure S8. (a) SHG intensity of $\text{Cs}_5\text{P}_5\text{Se}_{12}$ at 712 nm versus particle size and (b) relative SHG intensities of AgGaSe₂ (triangle) and crystalline (filled circle) and glassy (square) $\text{Cs}_5\text{P}_5\text{Se}_{12}$.

(a)



(b)



S9. Selected bond distances (\AA) for $\text{Cs}_5\text{P}_5\text{Se}_{12}$: P(1)-Se(1), 2.213(2); P(1)-Se(2), 2.156(2); P(1)-Se(3), 2.156(2); P(2)-Se(4), 2.162(2); P(2)-Se(5), 2.280(2); P(2)-Se(6), 2.121(2); P(3)-Se(5), 2.349(2); P(1)-P(2), 2.257(2). Selected bond angles (deg) for $\text{Cs}_5\text{P}_5\text{Se}_{12}$: Se(1)-P(1)-Se(2), 112.41(9); Se(1)-P(1)-Se(3), 113.35(9); Se(2)-P(1)-Se(3), 115.14(8); Se(1)-P(3)-Se(5), 89.97; Se(5)-P(3)-Se(5'), 100.67; Se(1)-P(3)-Se(1'), 178.02(13); P(1)-P(2)-Se(4), 108.22(9); P(1)-P(2)-Se(5), 99.70; P(1)-P(2)-Se(6), 112.80(9).

Selected bond distances (\AA) for $\text{Cs}_4\text{P}_6\text{Se}_{12}$: P(1)-Se(1), 2.303(2); P(1)-Se(2), 2.137(2); P(1)-Se(3), 2.140(2); P(2)-Se(4), 2.128(2); P(2)-Se(5), 2.127(2); P(2)-Se(6), 2.281(2); P(3)-P(3'), 2.232(2). Selected bond angles (deg) for $\text{Cs}_4\text{P}_6\text{Se}_{12}$: Se(1)-P(1)-Se(2), 111.26(9); Se(1)-P(1)-Se(3), 107.74(9); Se(2)-P(1)-Se(3), 116.42 (8); P(2)-P(1)-Se(1), 100.29(9); P(2)-P(1)-Se(2), 111.44(8); P(2)-P(1)-Se(3), 108.43(9).

References:

1. Canlas, C. G.; Muthukumaran, R. B.; Kanatzidis, M. G.; Weliky, D. P., *Solid State Nucl. Magn. Reson.* **2003**, 24, 110-122.
2. Gave, M.; Malliakas, C. D.; Weliky, D. P.; Kanatzidis, M. G., *Inorg. Chem.* **2007**, 46, 3632-3644.
3. McCarthy, T.; Kanatzidis, M. G., *J. Alloys Compd.* **1996**, 236, 70-85.
4. Chung, I.; Karst, A. L.; Weliky, D. P.; Kanatzidis, M. G., *Inorg. Chem.* **2006**, 45, 2785-2787.
5. Pregosin, P. S.; Kunz, R. W., *p31 sP and p13 sC NMR of transition metal phosphine complexes*. Springer-Verlag: Berlin ; New York, 1979; p 156 p.
6. Perera, S. D.; Shaw, B. L., *J. Chem. Soc. Chem. Commun.* **1995**, 865-866.
7. Canlas, C. G.; Kanatzidis, M. G.; Weliky, D. P., *Inorg. Chem.* **2003**, 42, 3399-3405.